Research Article

Advances in Mechanical Engineering

Advances in Mechanical Engineering
2015, Vol. 7(7) 1–14

DOI: 10.1177/1687814015592561
aime.sagepub.com
SAGE

Computational fluid dynamics and particle image velocimetry assisted design tools for a new generation of trochoidal gear pumps

M Garcia-Vilchez[1], PJ Gamez-Montero[1], E Codina[1], R Castilla[1], G Raush[1], J Freire[2] and C Río[2]

Abstract

Trochoidal gear pumps produce significant flow pulsations that result in pressure pulsations, which interact with the system where they are connected, shortening the life of both the pump and circuit components. The complicated aspects of the operation of a gerotor pump make computational fluid dynamics the proper tool for modelling and simulating its flow characteristics. A three-dimensional model with deforming mesh computational fluid dynamics is presented, including the effects of the manufacturing tolerance and the leakage inside the pump. A new boundary condition is created for the simulation of the solid contact in the interteeth radial clearance. The experimental study of the pump is carried out by means of time-resolved particle image velocimetry, and results are qualitatively evaluated, thanks to the numerical simulation results. Time-resolved particle image velocimetry is developed in order to adapt it to the gerotor pump, and it is proved to be a feasible alternative to obtain the instantaneous flow of the pump in a direct mode, which would allow the determination of geometries that minimize the non-desired flow pulsations. Thus, a new methodology involving computational fluid dynamics and time-resolved particle image velocimetry is presented, which allows the obtaining of the instantaneous flow of the pump in a direct mode without altering its behaviour significantly.

Keywords

Trochoidal gear pump, interteeth clearances, time-resolved particle image velocimetry, experimental characterization, instantaneous flow, computational fluid dynamics, flow visualization

Date received: 16 February 2015; accepted: 10 April 2015

Academic Editor: TH New

Introduction

The complicated aspects of the operation of a gerotor pump make computational fluid dynamics (CFD) the proper tool for modelling and simulating its flow characteristics. Furthermore, results from the numerical simulation can be used in order to complement dynamical simulation models (computationally much less expensive), thus allowing the analysis of the leakage effects in the overall behaviour of the pump.

In the literature, there are plenty of works based on CFD, but very few are aimed at positive volumetric

[1]Laboratorio de Sistemas Oleohidráulicos y Neumáticos (LABSON), Department of Fluid Mechanics, Universitat Politècnica de Catalunya, Terrassa, Spain
[2]Laboratorio de Sistemas Oleohidráulicos y Neumáticos (LABSON), Department of Mechanical Engineering, Universitat Politècnica de Catalunya, Terrassa, Spain

Corresponding author:
M Garcia-Vilchez, Laboratorio de Sistemas Oleohidráulicos y Neumáticos (LABSON), Department of Fluid Mechanics, Universitat Politècnica de Catalunya, Campus de Terrassa, Colom 11, 08222 Terrassa, Spain.
Email: mercedes.garcia-vilchez@upc.edu

displacement machines (Iudicello and Mitchell[1]), and in general there is a gap in the implementation of these studies and knowledge into trochoidal gear pumps. However, we must highlight the work done by Natchimuthu et al.[2] that optimizes the design of the intake channel in a gerotor pump, not considering the effects of cavitation in the suction line.

CFD models of gerotor pumps have been used to improve gerotor designs in many engineering applications for the last decades, but it was not until 10 years ago that CFD has been widely implemented. Regarding the first CFD publications related to gerotor pumps, in 1997 Jiang and Perng[3] created the first full three-dimensional (3D) transient CFD model for a gerotor pump and included a cavitation model. Their model successfully predicted gerotor pump volumetric efficiency losses due to cavitation. Kini et al.[4] couple CFD simulation with a structural solver to determine deflection of the cover plate in the pump assembly due to variation in internal pressure profiles during operation. Zhang et al.[5] study the effects of the inlet pressure, tip clearance, porting and the metering groove geometry on pump flow performances and pressure ripples using CFD model. Natchimuthu et al.[2] and Ruvalcaba and Hu[6] also use CFD to analyse gerotor oil pump flow patterns. Jiang et al.[7] create a 3D CFD model for crescent pumps, a variation of gerotor pumps with a crescent-shaped island between the inner and outer gears.

Ruvalcaba and Hu[6] develop a 3D CFD methodology to predict the flow performance and pump flow deficiency exhibited in gerotor pumps at different operation conditions. It is shown that cavitation has a non-significant influence on the pump flow deficiency and that tip-to-tip clearance has a critical impact on flow deficiency: imperative attention must be displayed towards the manufacturing tolerances of the gerotor pump. Choi et al.[8] develop an automated program for designing a gerotor and suggested that inserting a circular-arc curve between the hypocycloid and epicycloid curves controls the tip width of the inner rotor. Such insertion eliminates any upper limit on the eccentricity. Choi and colleagues also use a commercial CFD model to calculate flow rate and flow rate irregularity.

Ding et al.[9] describe a full 3D transient CFD model for an orbital gerotor motor. A moving/deforming mesh algorithm was introduced and implemented in the commercial CFD software package PumpLinx. It does not account for the mechanical and friction losses.

One aspect that is not already resolved is the complete leakage model that properly describes the real behaviour of the pump by properly simulating the contact point between each pair of teeth of the trochoidal profiles. Motivated by this fact, this article presents a 3D CFD model planned to accomplish this objective of clarifying how leakage flow affects the response of the pump. As a consequence, the model includes tolerances between the different pieces that integrate the gerotor pump and establishes the contact points between trochoidal profiles as a fluid-dynamic condition.

From the point of view of the experimental study of the gerotor pump, since it is practically impossible to measure accurately and directly the flow ripple generated by the pump, indirect measurements should be used, that is, measurements of pressure pulses and estimating the flow ripple with the help of an algorithm. Edge and Johnston[10] propose a methodology for the calculation algorithm of the flow ripple. Nevertheless, these pressure pulses generated by the pump have an interaction also with its own installation. As a consequence, the study of the same pump in different installations could lead to very different pressure pulsations. Named Secondary Source Method, this test method for measuring the source flow ripple and source impedance is based on the analysis of the wave propagation characteristics in a circuit which includes the pump under test and an additional source of fluid-borne noise.

Regarding the flow visualization techniques applied in gerotor pumps, only one reference has been found: Itoh et al.[11] carry out a study of the flow structure and the volumetric efficiency using light-reflecting tracer particles in a transparent model of the pump of external dimensions of 76.8 mm and a maximum rotating velocity of 31 r/min. And particularly about time-resolved particle image velocimetry (TRPIV), developed in the present work, there is no documented work of this procedure applied to trochoidal gear pumps. The first approach of this technique in gerotor pumps was first developed by Garcia-Vilchez,[12] as a work prior to the present.

Expanding the experimental study to the entire range of gear pumps, Ertürk et al.[13] study the characteristics of the flow pattern inside the suction chamber of an external gear pump for different gear pump angular velocities to investigate the turbulence effect of rotating gears on the system. In a later work, Ertürk et al.[14] study the flow characteristics of an external gear pump with TRPIV, performing measurements for different spatial resolution configurations and estimating the turbulent kinetic energy dissipation rate.

Besides, in Castilla et al.,[15] TRPIV measurements performed in an external gear pump with decompression slot are compared with the results obtained through a 3D numerical simulation of the pump.

In the first method, a pressure transducer is directly facing the volume between two vanes; in the second method, the sensor is located inside an external chamber where the oil is transferred via a duct suitably designed in the rotor shaft.

The only actual method to validate a new design of trochoidal gear pump is to perform a test in normal operating conditions of the real pump. According to

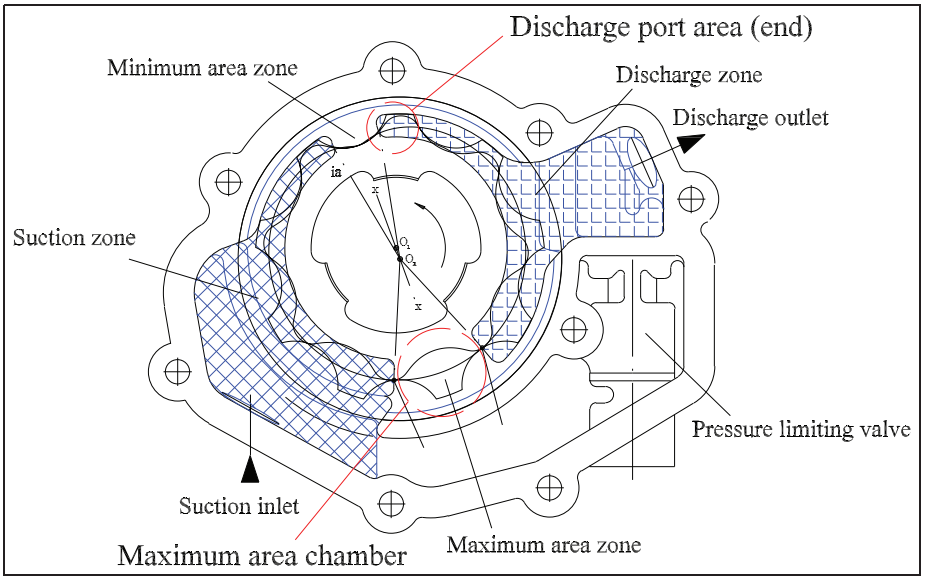

Figure 1. Gerotor pump and areas of study.

the documented work, there is no existing procedure to obtain the flow ripple generated by the pump in a direct and accurate measure. The experimental study by means of particle image velocimetry (PIV) could give further and accurate information of the fluid-dynamic real behaviour of the fluid inside the pump, as it could allow the obtaining of the instantaneous flow of the pump in a direct mode and without altering its behaviour significantly.

Geometry of study

The study is performed in two particular areas of the gerotor pump: the discharge port area zone and the maximum area chamber zone, shown in Figure 1.

Effective port areas are very important to be studied in gerotor pump design, as these areas have a direct influence on the overall performance of the pump. The instantaneous flow rate is influenced by the change in volume of the chambers, which in turn depends on the geometry of the port areas. Modifying the geometry of the area that connects each chamber with the suction or discharge zone, it is possible to reduce the flow rate irregularity, improving thereby the performance of the gerotor pump. In Gamez-Montero et al.,[16] it is found that little variations in the port areas produce important differences in the flow ripple of the pump. For the studied geometries in this work, it is seen that some of them produce a significant quantitative reduction in the irregularity flow index that can be almost about 12%. Flow irregularity measures the flow ripple generated by the pump, and by reducing this index, the life of both the pump and the installation can be extended, as phenomena like fatigue are attenuated.

On the other hand, the volumetric capacity is related with the pump's efficiency, and increases in this particular index result in a higher efficiency of the pump. The volumetric capacity of the pump can be determined by properly integrating the flow that crosses the maximum area chamber (the chamber that is located between the end of the suction port area and the start of the suction port area).

Regarding this study, another important aspect to consider is that results corresponding to the current scale of most of the trochoidal pumps used in industrial applications cannot be extrapolated directly to the mini-scale gerotor pumps. Thus, this work aims to develop and validate the TRPIV technique in trochoidal gear pumps, with the future objective of taking a step forward to the mini-scale gerotor pump.

Experimental study

As it is virtually impossible to measure accurately and directly the volumetric flow in any passage of the pump, indirect measures are used in order to characterize its instantaneous flow. These are measurements of pressure pulses, and the flow ripple is estimated with the help of an algorithm. According to the documented work published to date, the only method to validate a new design of trochoidal gear pump is to perform a test in normal operating conditions of the real pump. Moreover, there is not an existing procedure to obtain the flow ripple generated by the pump in a direct and accurate measure.

The experimental work presented in this article is aimed at the improvement of the TRPIV applied to positive displacement pumps and specifically to

trochoidal gear pumps. The effort made in this field is focused in order to make progress in this experimental technique, knowing its limitations as a new technique in development with respect to trochoidal gear pumps. It should not be interpreted as the validation of the theoretical models as the use of TRPIV in trochoidal gear pumps is not fully developed and the limitations of its use must be taken into account.

TRPIV is used in order to obtain the temporal evolution of the velocity field of the unsteady flow in every studied passage of the pump. This technique combines PIV and high-speed photography, recording a complete set of frames during a specific period of time.

The results obtained through TRPIV help the understanding of the real behaviour of the pump, as it is possible to obtain a whole velocity field in a particular section of the pump. Even the 3D velocity field could be analysed, which would be very useful in order to study the influence of the geometry of the port areas in a real pump.

Tracer particles

The selected tracer particles are alginate tracer particles designed and produced at the Rovira i Virgili University of Tarragona by Ertürk Düzgün.[17] Alginate particles present excellent flow seeding and light scattering abilities. They ensure good tracking of the fluid motion in both liquid and gas measurements. When they are used in liquid, there is not much difference in the density between the fluid and the particles, thanks to their porous structure that easily absorbs the analysing fluid. Also, alginate particles have soft, jelly-like structure and do not cause any damage to the inner contact surface of the machines. More details are given in Ertürk et al.[18] where it is demonstrated that alginate particles are very appropriate for turbo-machinery application in PIV, with mineral oil as the working fluid.

Alginate particles used in this study have an average diameter of 50 μm (Figure 2), and its concentration in the mineral oil is set to 0.375 g/L. In order to set the appropriate concentration in the system, the mineral oil is filtered to remove particles larger than 50 μm, and the particles are added progressively. In every new addition of particles to the system, the concentration is verified to be suitable, thanks to the PIV validation software in order to ensure that the density of particles in the recorded frames is between 5 and 15 particles in an interrogation area (32 × 32 pixels), which ensures a high probability of good analysis results.

Test bench and operating conditions

The pump has been experimentally studied with TRPIV in a test bench (Table 1). Due to the chosen experimental technique, it has been necessary to modify the casing of the pump and the outer gear wheel, in order to allow light to cross the chambers where the flow has to be filmed. The 3D design and the new casing made in methacrylate are seen in Figure 3.

In addition to the pump and the oil tank, a pressure-limiting valve is added in the discharge of the pump. The tank is situated 1 m above the pump, and no additional pressure is imposed in the discharge of the pump.

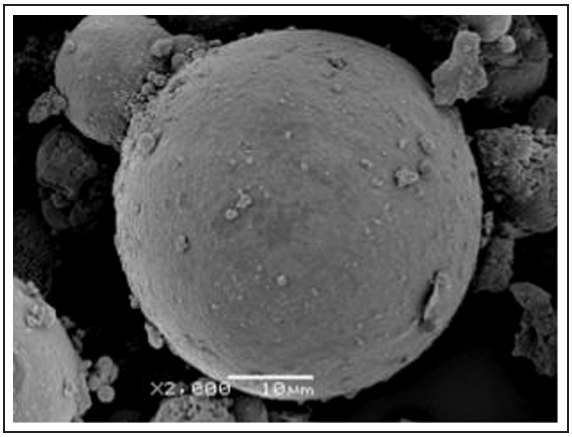

Figure 2. SEM images of alginate particles in dry form.

Table 1. Characteristics of the experimental testing.

High velocity camera	
Frame rate	3000 fps
Spatial resolution	1024 × 1024 pixels
Record time	0.7 s/2048 frames
Laser	
Pulse length	50 μs
Beam dimensions	12 mm × 0.7 mm at output
Synchronizer	
Waveform	Square
Mode	Continuous
Frequency	3 kHz
Symmetry control	50%
Output level	$5V_{p\text{-}p}$
DC offset	0.0 V
Operating conditions of the pump	
Rotary velocity of the pump (inner wheel)	250 r/min
Suction/discharge pressure	0.01/0.02 MPa
Properties of the mineral oil	
Viscosity	2.8×10^{-2} Pa s
Density	885 kg/m^3
Tracer particles concentration	0.375 g/L
Software	
Data acquisition	Camera's own control software: Photron FASTCAM Viewer
Image pre-processing	ImageJ (open source)
Image interrogation	GPIV (open source)
Post-processing and graphical representation	MATLAB

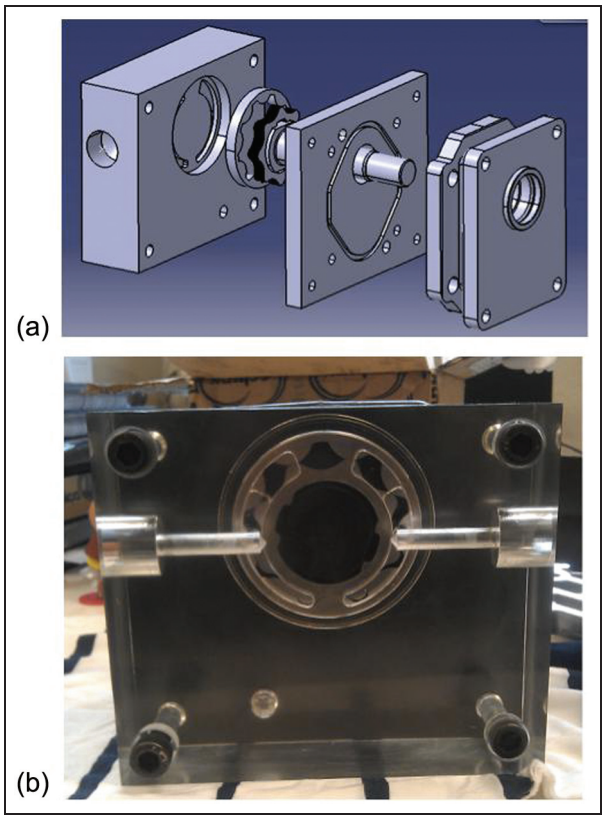

Figure 3. Modification of gerotor pump for the test bench: (a) 3D design and (b) assembly.

The estimated pressures in the suction and discharge connections are 0.1 and 0.02 MPa (gauge), respectively.

The chosen laser for the presented experiments was the Monocrom LU80250-FSAC. It is an 800-nm (infrared) laser. It is a diode laser, meaning that the active medium is a semiconductor similar to that found in a light-emitting diode that is powered by injected electric current. Laser diodes are arranged in a bar, making possible the production of the necessary laser sheet with optical elements that are encapsulated in the laser box. Therefore, the laser box is directly placed in front of the gear pump without the need for additional optical elements between laser and pump.

In order to acquire high-frequency time series of images in the TRPIV, the high-velocity digital camera that is used in the experiments is the Photron Ultima APX-RS. Its operating conditions are set to 3000 fps, with a spatial resolution of 1024 × 1024 pixels and a record time of 0.7 s (corresponding to 2048 frames).

Laser pulses have to be synchronized with the camera trigger using a synchronizer. In the case of TRPIV, the camera must be continuously triggered in order to generate each pair of frames to temporally resolve the flow. The Function Generator TG2000 20 MHz DDS has been used as the synchronizer between camera and laser. It can operate with standard waveforms of sine, square, triangle, DC, positive pulse and negative pulse, and in this study, the square waveform at continuous mode has been chosen.

In order to establish the rotary velocity during testing, some previous considerations about the temporal and spatial resolutions have to be defined. The high-speed digital camera allows recording up to 250,000 fps, but at very low spatial resolution (128 × 16 pixels). The selection of the temporal resolution of the experimental testing has been done selecting the maximum available frame rate at full resolution. The Photron Ultima APX-RS has a maximum spatial resolution of 1024 × 1024 pixels, and for this resolution the maximum available frame rate is 3000 fps. For these conditions, the buffer memory of the camera allows us to record up to 2048 images.

The size of the interrogation areas during evaluation must be small enough for the velocity gradients not to have significant influence on the results. Furthermore, it determines the number of independent velocity vectors and therefore the maximum spatial resolution of the velocity map, which can be obtained at a given spatial resolution of the sensor, employed for recording. According to the PIV bibliography and the recommendations in the software's user guide, the size of the interrogation area has been defined as 32 × 32 pixels.

The maximum rotary velocity (inner gear wheel, expressed in r/min) is defined by

$$\omega_{i,\,max}\ (\mathrm{rpm}) = \frac{20 \cdot IA\ (\mathrm{pixel}) \cdot SC\ (\mathrm{mm/pixel}) \cdot TS\ (\mathrm{s}^{-1})}{D_{ei}\ (\mathrm{mm})\pi} \tag{1}$$

where IA is the size of the interrogation area (32 × 32 pixels), SC is the spatial scale (0.035 mm), TS is the time scale (3000 fps) and D_{ei} is the external diameter through the tips of the teeth of the inner gear (65.45 mm); equation (1) leads to a maximum internal rotary velocity of approximately 327 r/min. Considering this maximum value and defining the operating rotary velocity as 75% of this maximum value, the selected value corresponds to 250 r/min.

Numerical simulation

As seen in the 'Introduction' section, one aspect that is not already resolved is the leakage model that properly describes the real behaviour of the pump. Motivated by this fact, the 3D CFD model is planned to accomplish this objective of clarifying how leakage flow affects the response of the pump. As a consequence, the model includes tolerances between the different pieces that integrate the gerotor pump, so the fluid-dynamic characteristics of its behaviour can be properly analysed.

Due to the dependence of the instantaneous flow regarding the teeth contact, a new boundary condition

Table 2. Geometry, operation conditions and fluid properties of the computational fluid dynamics (CFD) simulations.

Geometry and operation conditions of the numerical simulation	
Eccentricity	2.85 mm
External diameter through the tips of the teeth of the inner gear	65.45 mm
Radius of the circle to complete the outer gear	35.8 mm
Gear thickness	9.25 mm
Arc radius of the outer gear tooth	10.85 mm
Number of outer teeth	9
Number of inner teeth	8
Inlet gauge pressure	0 MPa
Outlet gauge pressure	0.054 MPa
Inner gear angular velocity	250 r/min
Volumetric capacity	9.8 cm^3/rotational speed
Properties of the mineral oil	
Density	885 kg/m^3
Viscosity	2.8×10^{-2} Pa s
Compressibility coefficient	1.5×10^{-9} Pa

called *gearing contact point* has been developed to simulate the teeth contact in the interteeth radial clearances through a fluid-dynamic condition, thus creating a virtual wall. This new boundary condition is integrated in the 3D model of the gerotor pump at every time step by means of a home-made ad hoc code.

The CFD simulations have been performed with the commercial code ANSYS FLUENT™ 12.0.16, based on the finite-volume method. The 3D modelling of the pump and its meshing have been done with the GAMBIT software package, which is a meshing software of FLUENT.

In order to be able to compare the results of the numerical simulation and the experimental study, the discharge pressure imposed in the CFD simulation has been increased to 54,000 Pa to force the simulation to increase leakage flow, thus equalling the flow in the outlet pipe between experimental and simulation results (Table 2).

Mesh characteristics

The computational domain of the fluid (Figure 4) is divided into three main zones: port area zones, gearing zone and base zone. As these zones are extrudable geometries, the 2.5-dimensional (2.5D) meshing technique is used. This technique is computationally less expensive than the regular volumetric meshing, compared to an equivalent volume of fluid.

The geometry of the port area zone has been meshed through hexahedral structured stationary mesh, and it includes the suction and discharge port area zones, and the suction and discharge tubes. The gearing zone is located between the gearing trochoidal profiles, and it is a triangular prism unstructured deforming mesh. To mesh this zone, it is necessary to scale the outer gear, and no contact between the inner gear and the outer gear profiles is established. The base zone geometry includes the radial clearance between the outer gear and the housing of the pump. It has been meshed through hexahedral structured stationary mesh.

Numerical simulations have been carried out through a dynamic mesh providing considerable mesh quality to the computation time. In order to update the volume mesh in the deforming regions subject to the motion defined at the boundaries, the spring-based smoothing method has been used, as employed in a similar geometry of gerotor pump in Gamez-Montero et al.[19]

From the available remeshing methods of ANSYS FLUENT, the 2.5D surface remeshing method has been chosen, as it is the one that fits with the 2.5D technique that has been used. Faces on a deforming boundary are marked for remeshing based on face skewness (set to 0.6), minimum and maximum length scales (set to 0.0001 and 0.0008, respectively) and an optional sizing function. If the faces are expanding, they are allowed to expand until the maximum length scale is reached. Otherwise, if the faces are contracting, they are allowed to contract until the minimum length scale is reached.

The deformation of the mesh is measured with the equivolume skewness of a cell, defined as

$$S_k = \frac{S_e - S_c}{S_e} \tag{2}$$

where S_c is the cell surface and S_e is the surface of an equilateral triangle with the same circumradius. In all the numerical simulations of this work, the maximum value of the area-averaged equivolume skewness S_k is below 0.89 for both the inter-profile surfaces, which is less than the value of 1 defined as a limit for a good mesh quality deformation.

Numerical schemes

The time derivative term in the balance equation of each physical magnitude is calculated with a first-order

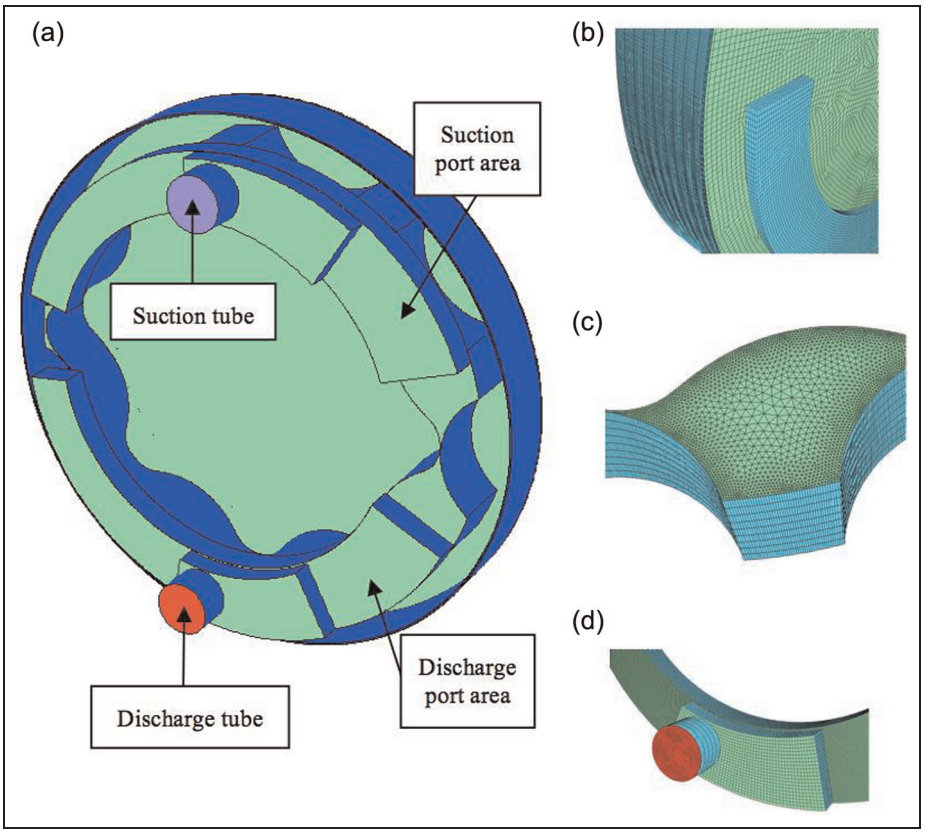

Figure 4. CFD domain: (a) general view, (b) base zone, (c) gearing zone and (d) port area zones.

implicit scheme, since this is the only method that our software allows with dynamic mesh. In the continuity equation, a second-order upwind scheme has been chosen in order to discretize the convective term, as it gives more accurate results than lower order schemes for triangular and hexahedral grids.

From the available algorithms, the pressure–velocity coupling scheme of Pressure-Implicit with Splitting of Operators (PISO) is chosen, as it is highly recommended in the software documentation for transient calculations on skewed meshes.

The spatial discretization of the momentum equations follows a high-order Quadratic Upstream Interpolation for Convective Kinematics (QUICK) scheme, which is based on a weighted average of second-order upwind and central interpolations of the variable. This scheme allows the calculation for a higher precision in the regions with structured mesh and becomes identical to the second-order upwind scheme in the rest of the computational domain. Furthermore, to discretize momentum equation, pressure values are needed on the control volume faces. Standard pressure discretization interpolates the pressure on the faces using the cell centre values. On the other hand, the pressure-staggered option (PRESTO) discretization for pressure actually calculates pressure on the face. This is possible using staggered grids where velocity and pressure variables are not 'co-located'. PRESTO discretization gives more accurate results since interpolation errors and pressure gradient assumptions on boundaries are avoided.

Turbulence modelling

The choice of turbulent model depends on considerations such as the physics contained in the type of flow, the level of accuracy required and the available computational resources, and the amount of time available for the simulation. The simplest complete models of turbulence are the two-equation models in which the solution of two separate transport equations allows the turbulent velocity and length scales to be independently determined.

From the available two-equation models in ANSYS FLUENT, the standard k–ε has been chosen, as it is the simplest turbulence model for which only initial and boundary conditions need to be supplied, it has an excellent performance for many industrially relevant flows and it is the most widely validated turbulence model.

As a semi-empirical model, based on model transport equations for the turbulent kinetic energy (k) and

its dissipation rate (ε), some constants and the turbulent Prandtl numbers have to be known, and they have been used as its default values: $C_{1\varepsilon} = 1.44$, $C_{2\varepsilon} = 1.92$, $\sigma_k = 1.0$ and $\sigma_\varepsilon = 1$.

Simulation of the tooth contact in the interteeth clearance

In order to model the manufacturing tolerance between the trochoidal profiles, the internal diameter of the outer gear is increased, and as a consequence, the two profiles do not share any contact point.

The solid contact point between the inner and outer profiles has been simulated using a leakage model based on the strategy developed in Gamez-Montero,[19] originally named *viscous wall cell*. First, the strategy finds the Z interteeth radial clearances having the minimum length. The wall cell that corresponds to the minimum distance between each pair of inner–outer gear teeth is searched through the mesh located at each interteeth radial clearance, and it is labelled as contact wall cell. Finally, the model enforces a high viscosity to each contact wall cell, thus creating a virtual wall as a solid–solid boundary condition. This process is done for every time step. To avoid numerical problems related to strong gradients, the cells within a small area around this position are also identified and a linear distribution of the viscosity is imposed in these cells, with the objective of gradually returning the viscosity to its normal value.

A home-made ad hoc code is used in order to apply this strategy to the numerical simulation. This code is programmed in C++ , and it is integrated in the CFD solver as a user-defined function (UDF), not included in the ANSYS FLUENT standard version.

In this work, this UDF used to calculate the contact points has been improved, in terms of calculation efficiency. A new strategy has been created, named *gearing contact point*. The main contribution has been the inclusion of the theoretical calculation of the contact points before searching in the domain of the fluid. The analytical coordinates of the contact points are calculated, for each angle of rotation of the gearing, which allows the calculation of the analytical contact angle, at each time step. By including this modification, the UDF reduces the number of cells in which it searches for the contact points, as a restriction has been introduced in the domain that forces the simulation to search only in the nearby cells corresponding to the coordinates of the contact point. This means that the function is only searching in the faces around the theoretical contact point. It can search as close to the theoretical contact point as we define in the code, by means of an angular tolerance ($\pm\delta\alpha$) included in the algorithm. The only condition that has to be considered to define $\delta\alpha$ is that it has to be able to contain the minimum number of cells where we want to impose the linear distribution of viscosity.

Another improvement introduced, thanks to the gearing contact point strategy, is that it is not necessary to search in all the faces of outer and inner profiles, so reducing strongly the calculation time of the simulations. Once a cell of the outer profile is located inside the neighbouring of the theoretical contact point, it is labelled as contact wall cell.

The pseudo-code of the original algorithm and the modified one are presented in Figure 5. The comparison of the calculation between the two strategies corresponds to a calculation of a laminar case, with a time step of 3×10^{-5} s, performed with an Intel® Pentium® Dual CPU E2200 @ 2.20 GHz × 2 with a RAM memory of 1.9 GiB. Results show a reduction in calculation time of about 40% comparing gearing contact point and viscous wall-cell strategies.

Results and discussion

The experimental results are qualitatively evaluated, thanks to the numerical simulation results. And with respect to the understanding of the comparison between experimental and simulation results, it must be taken into account that the experimental study has been performed in a gerotor pump made of methacrylate. In addition, the diameter of the chasing has been increased with respect to the original pump, in order to reduce wear of the outer gear wheel.

On the one hand, as studied by Biernacki and Stryczek,[21] from the viewpoint of hydraulics, during the pumping action the condition of deformations is more important than the condition of stresses. This is so because, by keeping the stresses lower than acceptable, it is at the same time possible to achieve deformations and clearances greater than the extreme, which causes flaws in the pumping process, as well as lowering of the working pressure and pump efficiency. On the other hand, the increase in the clearance between outer gear and chasing results in a higher leakage flow. As a consequence, the results of the numerical simulation and experimental results cannot be compared directly, as there is more leakage in the tested pump, due to increased clearance and deformation in the methacrylate parts. In order to be able to compare the results, the discharge pressure imposed in the CFD simulation has been increased to 54,000 Pa to force the case to increase leakage flow, thus equalling the flow in the outlet pipe between experimental and simulation results. In order to characterize the type of flow in this study, a Reynolds number is defined as

$$\mathrm{Re} = \frac{\rho v d_o}{\mu} = \frac{4\rho Q}{\mu \pi d_o} \tag{3}$$

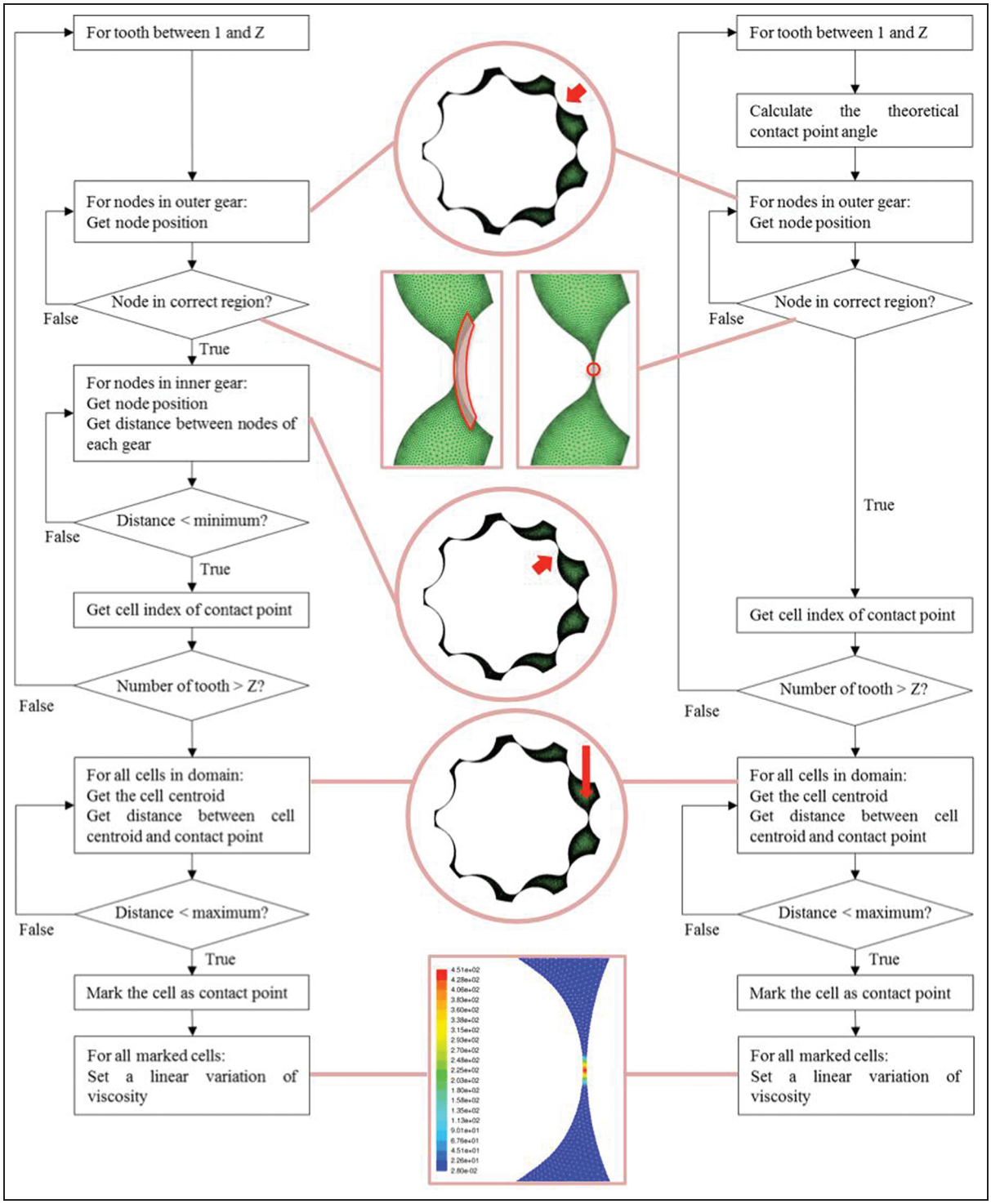

Figure 5. Pseudo-code of the viscous wall-cell strategy (left) and gearing contact point strategy (right).

where ρ and μ are the density and dynamical viscosity of the fluid, respectively; v and Q are the average velocity and the flow rate at the outlet pipe, respectively; and d_o is the diameter of the outlet port pipe. In this work, for an angular velocity of 250 r/min and considering the theoretical flow, the Reynolds number is $\mathrm{Re} \approx 183$, which is a value showing a laminar flow condition.

In order to obtain the results corresponding to the experimental study, each pair of experimental frames is evaluated, thanks to the open source GPIV software which runs through Bash scripts as it does not allow

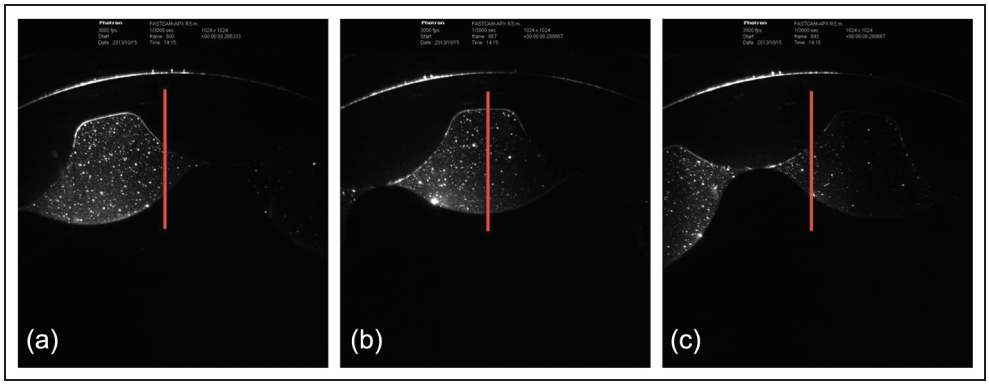

Figure 6. PIV image – maximum area chamber and flow plane calculation: (a) $T/T_g = 0.25$, (b) $T/T_g = 0.50$ and (c) $T/T_g = 0.75$.

working with graphical interface commands in the TRPIV interrogation. The evaluation of the experimental data by means of GPIV provides the two components of velocity for each of the coordinates contained inside the area of interest. GPIV is a Graphic User Interface program for the interrogation, validation and post-processing of the PIV data. It is an open source code created by Van der Graaf.[20]

The image pre-processing has been performed using the ImageJ software.[22] ImageJ is an open source code written in Java, which can be run on Linux, Mac OS X and Windows. It has an extended community of users, and it supports a wide range of image file formats, allowing the user to work with image sequences, so it is possible to process all the images obtained in a PIV as a package.

The flow ripple in the maximum area chamber can be obtained integrating the velocity vectors that cross a vertical plane centred in the width of the chamber (Figure 6). This is done in MATLAB, and the result is instantaneous flow for the complete set of experimental frames. This same procedure is used in the discharge port area, for a vertical plane placed in the radial direction of the external circumference defining the port area outline. Unlike the case of the maximum area chamber, the experimental frames have to be rotated prior to the PIV interrogation in order to achieve a vertical position of this plane.

Apart from the estimation of the instantaneous flow in the studied areas, MATLAB can also be used to graphically represent the velocity vector field, the contours of velocity and the streamlines. Figure 7 presents an example of the graphical depiction of the experimental results, belonging to the maximum area chamber, for a rotation angle of the outer gear of 90° and 270°, with respect to its reference position. It contains the velocity vector field representation, as well as the contours of velocity in connection with the velocity field. Also, the vector velocity field obtained through PIV measurements is compared with the one calculated by means of the CFD simulation.

The results are presented in the figures using the normalized values of flow Q/Q_g and time T/T_g. The time has been normalized with the gearing period T_g, which is the time that is needed for the tooth meshing to be repeated.

The calculated flow corresponds to a flow per unit of depth (m^2/s). This flow is obtained by integration of the vector field (PIV or CFD) across a fixed plane. It is not a volumetric flow, as the information obtained through the experimental study is limited to the velocity vectors contained in a plane. Consequently, the value of Q_g that is used to normalize the flow results corresponds to the theoretical flow (at the working rotary velocity of 250 r/min) per unit of depth of the gearing, that is, $4.41 \times 10^{-3}\,m^2/s$.

Figure 6 shows examples of PIV experimental frames obtained for the maximum area chamber and also the plane that has been established for the calculation of flow. In Figure 8, an example of PIV experimental frame obtained for the end of the discharge port area can be seen, in addition to the plane for the flow calculation in this area. In this case, the experimental frames have to be rotated before the PIV evaluation. This rotation is necessary as the PIV evaluation of the experimental frames generates a rectangular grid of the velocity vectors in the interrogation area. Then, it is only possible to estimate the flow crossing a vertical or horizontal plane using one of the two components of the velocity. Accordingly, if the flow crossing a plane at a certain angle is needed, the experimental frames have to be rotated this particular angle before its PIV evaluation.

Figure 9 shows the evolution of the flow in the maximum area chamber for the experimental study and the numerical simulation. What is really interesting of these results is that there is a clear correspondence between the experimental and the numerical results, as the two flow responses have the same tendency, both having the same order of magnitude. As can be seen, the experimental flow never reaches the zero value due to the leakage flow of the tested pump.

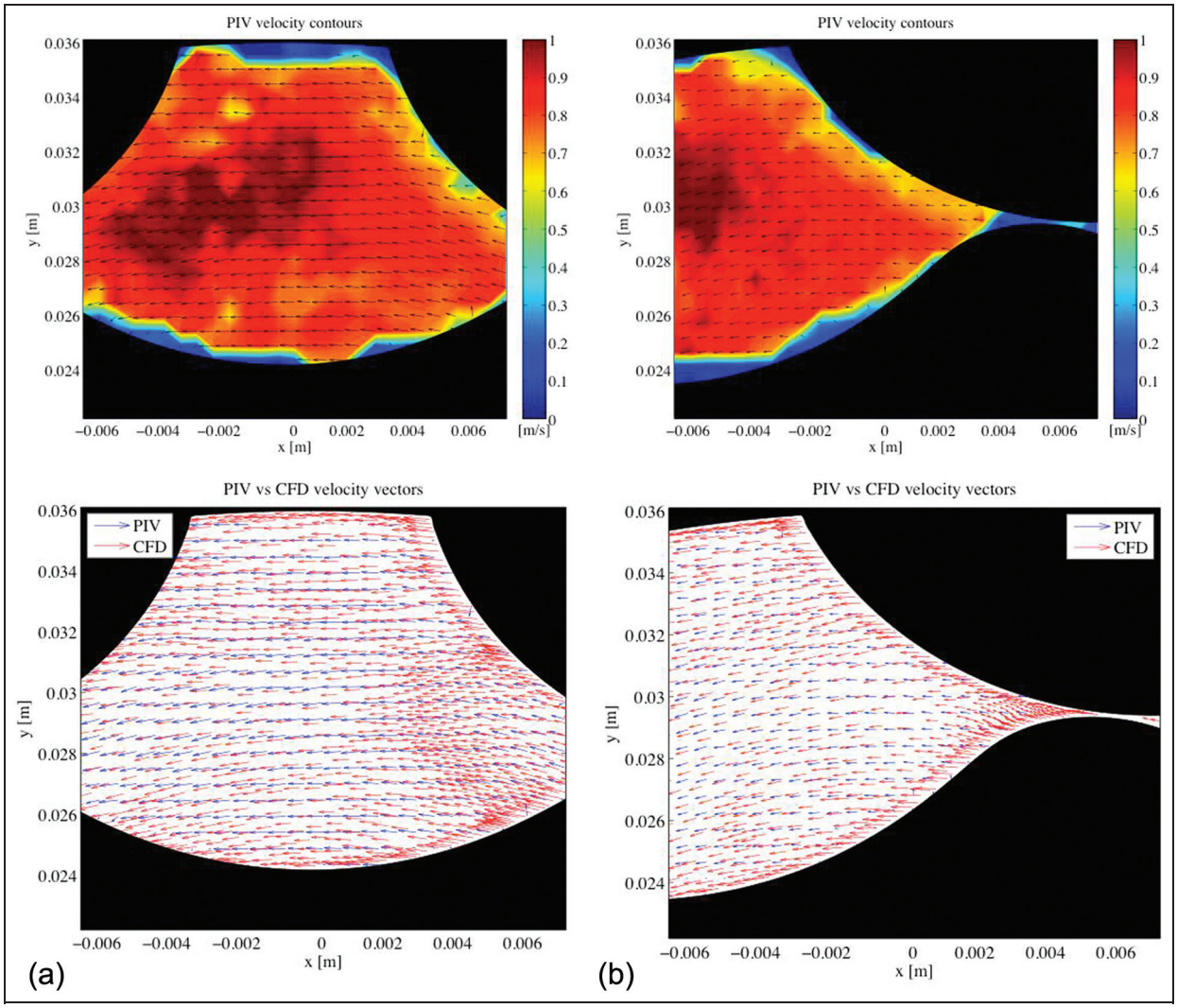

Figure 7. PIV contours and comparison of velocity vector field between PIV and CFD: (a) $T/T_g = 0.25$ and (b) $T/T_g = 0.50$.

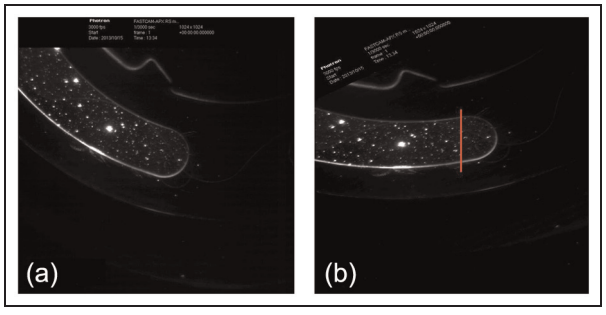

Figure 8. PIV image – discharge port area: (a) original image and (b) rotated image with plane for flow calculation.

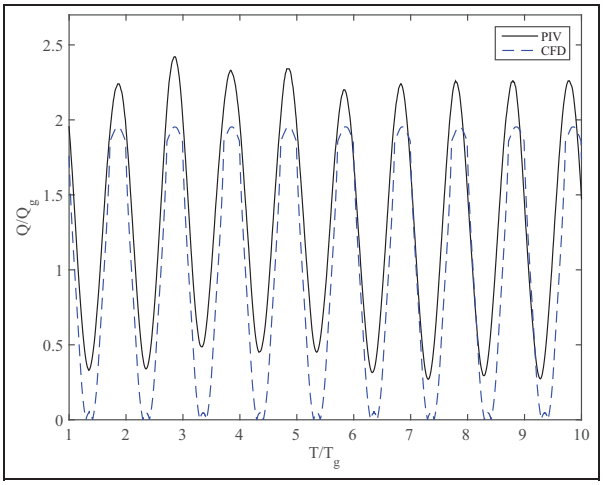

Figure 9. PIV and CFD (fixed centres) flow in the maximum area chamber.

Figure 10 shows the evolution of the flow at the end of the discharge port area for the experimental study and the numerical simulation. It can be seen that the

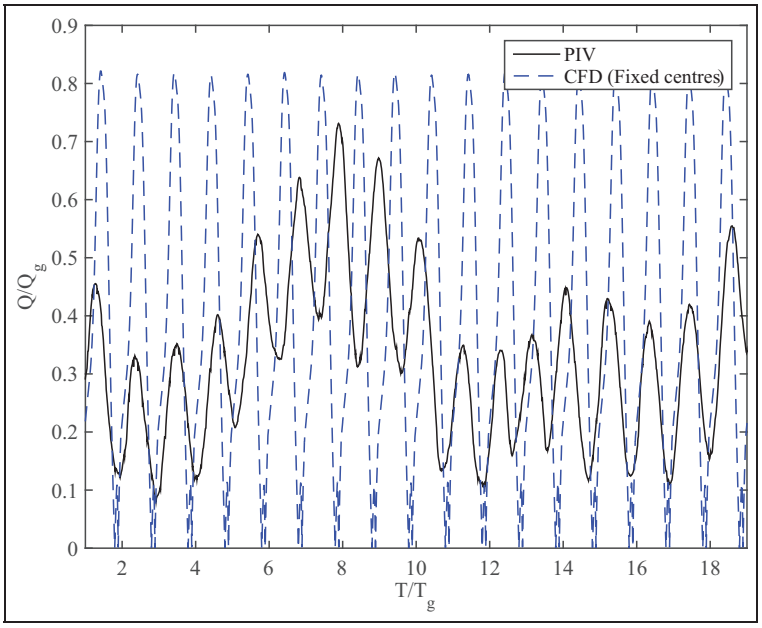

Figure 10. PIV and CFD (fixed centres) flow in the discharge port area.

flow pulsations correspond to a complete rotation of the gearing (nine pulsations corresponding to the nine teeth), for both the simulation and experimental results. It can also be observed that, in the experimental data, there is another main pulsation superposed to the nine pulsations of teeth. This may probably be caused by the relative movement between the centres of the gears in the real pump, as due to the increased tolerances, the centre of the outer wheel does not remain constant. In order to check whether this secondary pulsation may be caused by the movement between the centres, a new CFD simulation is conducted: in this case, the centres of the gears do not remain fixed, but the centre of the inner gear wheel moves in the x axis (see Figure 1) in a sinusoidal movement with 100 μm amplitude. This value of amplitude is properly chosen in order to avoid mesh interaction between the gearing zone and the base zone, and it also corresponds to the average manufacturing tolerance of the pump. Results of this simulation show a clear influence of simulating with relative movement between centres (Figure 11).

These results also show that numerical simulation achieves higher values of volumetric flow, compared to the experimental results. It may be understood as a consequence of the modifications of the pump in order to adapt it to the experimental requirements: due to increased clearance and deformation in the methacrylate parts, there is more leakage in the tested pump, so there is less working fluid crossing the fixed plane in the outer port area, as the velocity components of the fluid in other directions are greater in the case of experimental results than in the numerical simulation.

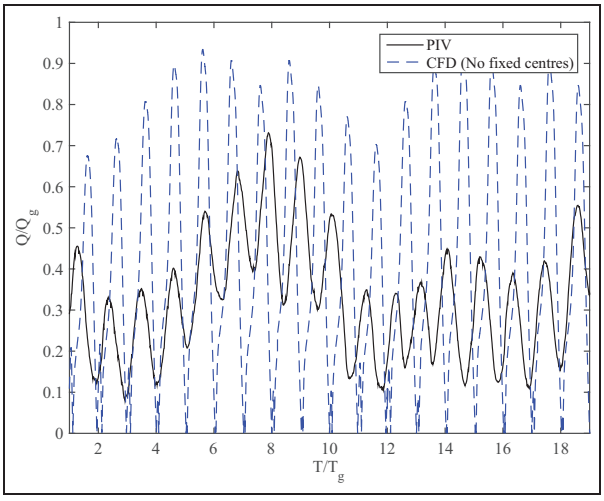

Figure 11. PIV and CFD (no fixed centres) flow in the discharge port area.

Conclusion

A 3D numerical model considering leakage and manufacturing tolerance has qualitatively evaluated the TRPIV experimental data for the gerotor pump. The comparison shows good agreement, as both the simulation and experimental results have the same tendency in the flow behaviour, and they have the same order of magnitude. The existing differences can be explained by the effects of testing with a gearing mechanism made of methacrylate with increased tolerances and achieving deformations and clearances greater than the extreme, thus lowering the working pressure and pump efficiency.

The gearing contact point strategy represents a reduction of 40% of the calculation time, with respect to the previous strategy named viscous wall cell. This has been possible, thanks to the incorporation of the theoretical calculation of the contact point in the UDF that defines the solid contact points between trochoidal gears. Besides, this new UDF gives the value of the minimum radial clearance between teeth.

The experimental study by means of TRPIV has established a new methodology for the accurate determination of velocity fields inside the pump, as seen, thanks to the comparison with the numerical simulation. The experimental pump has been appropriately adapted to the experimental technique requirements: the casing and the gear have been made of methacrylate and tolerances between the moving pieces have been increased, in order to be able to film the tracer particles and to reduce wear, respectively.

The volumetric behaviour of the pump has been evaluated through the measured flow in the maximum area chamber. Results show a clear correspondence between the experimental and the simulation behaviour, as they both have the same tendency and the same order of magnitude.

Results of the volumetric flow at the end of the discharge port area have shown that, apart from the main frequency of pulsation for each tooth, a secondary oscillation is present in the experimental results. Comparing these results with a numerical simulation with no fixed centres of rotation, we see that this movement has a remarkable influence on the flow of the discharge port area.

This work was aimed to evaluate the possibility of establishing TRPIV as a tool for directly measuring the flow inside the pump, in a non-intrusive way, without adding any other components that modify its normal operation. Considering the results from this work, TRPIV is proved to be a feasible alternative to obtain the instantaneous flow of the pump in a direct mode and without altering its behaviour. It constitutes an alternative to the Secondary Source Method, and it is the first approach of TRPIV applied to a trochoidal gear pump, according to the authors' knowledge. The use of TRPIV would allow obtaining the instantaneous flow of the pump in a direct mode, which would allow the determination of geometries that minimize the non-desired flow pulsations.

The improvement of the TRPIV technique applied to gerotor pumps is left to future work in order to achieve its quantitative validation. Once it is validated in the presented scale of pumps, efforts will be focused on its adaptation to the mini-scale trochoidal gear pumps.

Acknowledgements

The authors gratefully acknowledge the lab technicians Justo Zoyo and Jaume Bonastre for providing laboratory resources and support in the experimental work. The authors would also like to acknowledge the support of Aplicaciones de Metales Sinterizados (AMES; Spain) and Pedro Roquet (Spain).

Declaration of conflicting interests

The authors declare that there is no conflict of interest.

Funding

This research programme, projects DPI2011-27938 and DPI2013-42031-P, received financial support from the Ministry of Economy and Competitiveness of Spain and is co-financed by FEDER funding of EU; the authors acknowledge these financial supports.

References

1. Iudicello F and Mitchell D. CFD modeling of the flow in a gerotor pump. In: Burrows CR and Edge KA. *Bath workshop on power transmission and motion control*. London: Professional Engineering Publishing, 2002, pp.53–66.
2. Natchimuthu K, Sureshkumar J and Ganesan V. CFD analysis of flow through a gerotor oil pump. SAE technical paper 2010-01-1111, 2010.
3. Jiang Y and Perng C. An efficient 3D transient computational model for vane oil pump and gerotor oil pump simulations. SAE technical paper 970841, 2002.
4. Kini S, Mapara N, Thoms R, et al. Numerical simulation of cover plate deflection in the gerotor pump. SAE technical paper 2005-01-1917, 2005.
5. Zhang D, Perng C and Laverty M. Gerotor oil pump performance and flow/pressure ripple study. SAE technical paper 2006-01-0359, 2006.
6. Ruvalcaba MA and Hu X. Gerotor fuel pump performance and leakage study. In: *Proceedings of the ASME 2011 international mechanical engineering congress & exposition*, Denver, CO, 11–17 November 2011, paper no. IMECE2011-62226. New York: ASME.
7. Jiang Y, Furmanczyk M, Lowry S, et al. A three-dimensional design tool for crescent oil pumps. SAE technical paper 2008-01-0003, 2008.
8. Choi TH, Kim MS, Lee GS, et al. Design of rotor for internal gear pump using cycloid and circular-arc curves. *J Mech Des Trans ASME* 2012; 134: 011005.
9. Ding H, Lu XJ and Jiang B. A CFD model for orbital gerotor motor. In: *Proceedings of the institution of mechanical engineers, 26th IAHR symposium on hydraulic machinery and systems*, Peking, Kina, 26 November 2012. DOI: 10.1088/1755-1315/15/6/062006.
10. Edge KA and Johnston DN. The 'secondary source' method for the measurement of pump pressure ripple characteristics, part 1: description of method. *Proc IME A J Power Energ* 1990; 204: 33–40.

11. Itoh T, Murai Y, Ueno Y, et al. Visualization of internal flow in an inscribed trochoid gear pump. *J Vis Soc Jpn* 2005; 25: 303–304.
12. Garcia-Vilchez M. *Design tools applied to a trochoidal gear pump*. PhD Thesis, Universitat Politècnica de Catalunya, Terrassa, 2014.
13. Ertürk N, Vernet A, Castilla R, et al. Experimental analysis of the flow dynamics in the suction chamber of an external gear pump. *Int J Mech Sci* 2011; 53: 135–144.
14. Ertürk N, Vernet A, Pallarès J, et al. Small-scale characteristics and turbulent statistics of the flow in an external gear pump by time-resolved PIV. *Flow Meas Instrum* 2013; 29: 52–60.
15. Castilla R, Gamez-Montero PJ, Del Campo D, et al. Three-dimensional numerical simulation of an external gear pump with decompression slot and meshing contact point. *J Fluid Eng* 2015; 137: 041105. DOI: 10.1115/1.4029223.
16. Gamez-Montero PJ, Garcia-Vilchez M, Raush G, et al. Relief grooves effects in a trochoidal-gear pump using new modules of GeroLAB. *J Mech Des Trans ASME* 2012; 134: 054502.
17. Ertürk Düzgün N. *Particle image velocimetry applications in complex flow systems*. PhD Thesis, Departament d'Enginyeria Mecànica, Universitat Rovira i Virgili, Tarragona, 2012.
18. Ertürk N, Düzgün A, Ferrè J, et al. Alginate flow seeding microparticles for use in Particle Image Velocimetry (PIV). In: *10th international symposium on particle image velocimetry (PIV13 2013)*, Delft, 1–3 July 2013.
19. Gamez-Montero PJ, Castilla R, Del Campo D, et al. Influence of the interteeth clearances on the flow ripple in a gerotor pump for engine lubrication. *Proc IME D J Automobile Eng* 2012; 226: 930–942.
20. Van der Graaf G. Gpiv: an open Source project for PIV. *Presentation at PIVNET/ERCOFTAC workshop*, Lisbon, 9–10 July 2004.
21. Biernacki K and Stryczek J. Analysis of stress and deformation in plastic gears used in gerotor pumps. *J Strain Anal Eng* 2009; 45: 465–479.
22. Rasband WS. *ImageJ*. Bethesda, MD: US National Institutes of Health, 1997–2012, http://imagej.nih.gov/ij/